Available online at www.sciencedirect.com

ScienceDirect

Neuromuscular Disorders 29 (2019) 533–542

www.elsevier.com/locate/nmd

Efficient gene transfer into primary muscle cells to analyze nerve-independent postsynaptic organization *in vitro*

Jessica Mella[a], Viviana Pérez[a], Diego Zelada[a], Nicolás Moreno[a], Ariel Ionescu[b], Eran Perlson[b], Juan Pablo Henríquez[a,*]

[a] *Faculty of Biological Sciences, Neuromuscular Studies Laboratory (NeSt Lab), Department of Cell Biology, Center for Advanced Microscopy (CMA BioBio), Universidad de Concepción, Casilla 160-C, 4089100 Concepción, Chile*

[b] *Department of Physiology and Pharmacology, Sackler Faculty of Medicine, Sagol School of Neuroscience, Tel Aviv University, Tel Aviv, Israel*

Received 21 December 2018; received in revised form 23 April 2019; accepted 17 May 2019

Abstract

Acetylcholine receptor (AChR) clustering on the surface of muscle cells is a hallmark of postsynaptic differentiation at the vertebrate neuromuscular junction (NMJ). Even though the assembly of complex postsynaptic apparatuses is known to rely on both, pre- and postsynaptic signals, the identity of muscle-derived proteins modulating postsynaptic assembly and maintenance is still to be fully elucidated. Efficient gene transfer into muscle cells represents a powerful tool to analyze the contribution of muscle proteins on postsynaptic assembly and maintenance. Here, we describe a protocol that combines efficient electroporation of primary muscle satellite cells with the formation of aneural complex postsynaptic structures on the surface of myotubes. *In vitro* formed postsynaptic structures share various similarities with *in vivo* postsynaptic NMJ domains. While primary myotubes express increasing amounts of the ε AChR subunit, associated with NMJ maturation, surface AChR aggregates lack this AChR subunit. Our results also validate the functional expression of a luciferase reporter gene, as well as the response of complex postsynaptic structures to pharmacological treatment. Together, these methods in primary muscle cells are a valuable tool to perform a detailed and accurate analysis of the potential role of muscle-derived proteins on the maintenance of complex postsynaptic structures and to identify nerve-derived signals regulating functional NMJ maturation.
© 2019 Elsevier B.V. All rights reserved.

Keywords: Acetylcholine receptor; Electroporation; Myoblasts; Myotubes; Postsynaptic.

1. Introduction

The establishment, maturation and maintenance of functional contacts between motor neurons and skeletal muscles at the neuromuscular junction (NMJ) are essential events for the coordinated movement of many organisms. The main morphological features leading to embryonic NMJ formation have been well described; axonal growth cones differentiate into presynaptic terminals, whereas the innervated portion of the muscle membrane aggregates acetylcholine receptors (AChRs) on its surface. At the mature NMJ, the postsynaptic terminal becomes drastically re-arranged to organize unique pretzel-like structures, which alternate domains having or not AChR aggregates [1,2]. Functional NMJ maturation is accomplished by the switch of pentameric $\alpha 2\beta\gamma\delta$ AChR subunits to a $\alpha 2\beta\varepsilon\delta$ configuration [3,4]. Dysfunctions of the NMJ are triggered by traumatic spinal cord injury, as well as by severe motor pathologies. In spite of the almost null regenerative ability of the central nervous system, the injured peripheral nervous system displays a high regenerative efficiency. However, this depends on the time frame of denervation and only occurs in innervation-permissive conditions. These conditions must ensure the maintenance of muscle postsynaptic apparatuses until they become re-innervated [5]. The muscle-derived molecules involved in the formation and/or maintenance of postsynaptic structures in the absence of presynaptic inputs have not been fully elucidated.

* Corresponding author.
E-mail address: jhenriquez@udec.cl (J.P. Henríquez).

https://doi.org/10.1016/j.nmd.2019.05.005
0960-8966/© 2019 Elsevier B.V. All rights reserved.

Several of the molecular mechanisms leading to postsynaptic differentiation at the NMJ have been dissected in studies involving *in vitro* cultures of muscle cells, being myotubes derived either from muscle cell lines or from primary muscle satellite cells the most commonly used models. For instance, the motor neuron-derived proteoglycan agrin induces the formation of small aggregates of AChRs and other postsynaptic proteins in cultured muscle cells [6,7]. Remarkably, complex postsynaptic structures, resembling those observed *in vivo*, can also be formed on the surface of C2C12 cells myotubes when they are cultured onto polyornithine/laminin matrices [8].

Gain- and loss-of-function experiments in cultured myotubes constitute a potent molecular strategy to study neurally-induced (*e.g.* agrin-dependent) or aneural (*e.g.* laminin-induced) postsynaptic differentiation at the NMJ. Non-viral electroporation of genes has proven a useful method to transfect primary muscle cells [9–11], but the ability of electroporated cells to fuse into myotubes and assemble postsynaptic structures has not been analyzed in detail. Here, we describe a simple methodological strategy that combines efficient electroporation-mediated gene expression in mouse primary muscle satellite cells with the formation of aneural complex postsynaptic structures on differentiated myotubes. Our proposed method constitutes a powerful screening procedure to study the potential role of muscle proteins on aneural postsynaptic assembly at the NMJ.

2. Materials and methods

2.1. Primary culture of muscle satellite cells

Our procedures have been approved by the Bioethics Committee at Universidad de Concepcion, Chile, and follow the norms imposed by the Bioethics Committee of the National Commission for Scientific and Technological Research, Chile (CONICYT). Satellite cells were routinely isolated from Gastrocnemius muscles of adult (6–10 weeks) mice, using methods modified from previous studies [12]. Briefly, the skin from hind limbs was removed and the gastrocnemius muscle was dissected from bones and incubated in 2 mg/ml collagenase I (Sigma) in DMEM containing 2.5% penicillin-streptomycin (PS) for 3 h at 37 °C. Myofibers were then triturated and incubated for 3–4 days in Matrigel-coated (ThermoFisher Scientific) six-well plates with Bioamf-2 medium (Biological Industries) with 1% PS at a density of 100–120 myofibers per well. For enrichment of the satellite cells population, adhered cells were trypsinized and pre-plated onto an uncoated dish for 1 h at 37 °C. Non-adherent cells were then transferred into a Matrigel-coated dish with Bioamf-2 medium with 1% PS. Pre-plating was performed for two to three consecutive days, maintaining the culture at less than 50% confluence. Cultures were maintained with Bioamf-2 medium with 1% PS in 37 °C and 5% CO_2.

2.2. Electroporation procedures

We setup transgenesis of satellite cells using the NEON® transfection system (ThermoFisher Scientific) following the instructions of the manufacturer, with some modifications. Briefly, a total of 3×10^5 cells were resuspended in resuspension buffer R plus the corresponding volume of the expression vector(s). A volume of 10 µl (one at a time) of this mixture was aspirated with the NEON® reaction tip using the electroporation pipette and positioned inside the electroporation tube containing 3 mL of the electrolytic buffer E. We considered three of the electroporation conditions suggested by the manufacturer: the one to transfect mouse C2C12 myoblasts (condition 1), and the two protocols suggested for rat L6 myoblasts (conditions 2 and 3). These protocols differ in the electric field as well as in the number and time of pulses (0.55 kV/cm, 3 pulses of 10 ms for condition 1; 0.42 kV/cm, 1 pulse of 30 ms for condition 2; and 0.37 kV/cm, 2 pulses of 30 ms for condition 3). We used three DNA concentrations in the mix (0.02, 0.05, and 0.1 µg/µl DNA) for each condition. Electroporated cells under the nine conditions were resuspended in an eppendorf tube containing fresh Bioamf-2 medium with 1% PS and then seeded in equivalent volumes onto multi-well dishes or coverslips, as needed.

2.3. Transfection efficiency and myoblast survival

Electroporated myoblast were seeded onto polyornithine/laminin coated dishes as described [8] and cultures were maintained in Bioamf-2 medium with 1% PS during 24 h at 37 °C and 5% CO_2. Myoblasts were then fixed in p-formaldehyde 2% for 20 min at 4 °C, followed by methanol for 5 min at −20 °C. Nuclei were stained with DAPI (300 nM, Molecular Probes). Transfected cells were imaged in a Nikon Eclipse 80i microscope. A total of 12 images per coverslip were captured and the proportion of electroporated cells was calculated as a percentage of the total nuclei. To evaluate cell survival, the number of nuclei in tdTomato-positive cells obtained after the nine electroporation conditions was compared with the number of nuclei counted in control non-electroporated cells.

2.4. Aneural complex AChR structures in primary myotubes and immunocytochemistry

Before reaching confluency, control non-electroporated and electroporated satellite cells were switched to differentiation medium (DMEM plus 10% horse serum, 10% Fetal Bovine Serum, 1% PS, 1% GlutamaxTM) and incubated at 37 °C, 5% CO_2 for 8 days before fixation in p-formaldehyde 2% for 20 min at 4 °C, followed by methanol for 5 min at −20 °C. Under these culture conditions aneural complex postsynaptic structures form spontaneously. To analyze complex postsynaptic structures, myotubes were stained for 30 min with 5 µg/mL Alexa488-conjugated α-bungarotoxin (BTX; ThermoFisher). Postsynaptic apparatuses were imaged

through *z*-stacks series, which were collected using a Zeiss LSM700 confocal laser-scanning microscope (CMA Bio-Bio, Universidad de Concepcion). Morphologies were categorized into four different shapes: (i) "cluster", corresponding to small (area $< 50\mu m^2$) and uniformly stained; (ii) "plaque", corresponding to bigger (area $> 50\mu m^2$) structures; (iii) "pretzel", which comprise postsynaptic structures having sub-regions of null AChR staining; and iv) "fragmented", where the postsynaptic structures are divided into three or more small islets of AChR clusters. The frequency of the different morphologies was compared in the different experimental conditions. Myotube surfaces were manually traced on bright field images and their area was calculated using the Image J software. The total area of myotubes was calculated as a fraction of the total area of myotubes. In some experiments, myotubes were treated with 10 mM lithium chloride or 200pM agrin for 18 h before fixation. For immunocytochemistry, fixed myotubes were incubated with the primary antibodies anti-rapsyn (1:500; Abcam) or anti c-myc (1:25, Santa Cruz Biotechnology) for 16 h at 4 °C, washed, and incubated with Cy2-conjugated anti-mouse or Cy3-conjugated anti-rabbit antibodies (1:300, Jackson ImmunoResearch Laboratories) for 2 h. Nuclei were counterstained with DAPI (300 nM, Molecular Probes) in the same incubation step. Coverslips were mounted with fluorescence mounting medium (DAKO). For immunohistochemistry, whole-mounted LAL muscles were dissected and fixed with 1.5% v/v formaldehyde (Merck) for 90 min, washed with PBS 1X containing 0.5% Triton X-100 (USBiological), blocked in PBS 1X, 0.5% Triton X-100 and 4% BSA for 16–18 h at 4 °C, and incubated with an anti rapsyn antibody (1:500, Abcam) for 16 h at 4 °C. After washing, samples were incubated with a Cy2-conjugated anti mouse antibody along with Alexa555-conjugated BTX, washed, and mounted with fluorescence mounting medium (DAKO).

2.5. Luciferase assay

For luciferase assays, 125 ng of the TOPflash reporter and 12.5 ng of the control *Renilla* luciferase gene were transferred to satellite cells by electroporating at 0.55 kV/cm, 3 pulses, 10 ms. Empty pBluescript plasmid was added in a sufficient amount to reach 0.05 μg/μl of total plasmid DNA per reaction mix. After 36 h, cells were treated with 50 mM lithium chloride for 15–20 h. Cells were subsequently lysed and the activity of the TOPflash and *Renilla* reporter genes were measured in a Victor 3 Luminometer (Perkin-Elmer) using the Dual Luciferase Report Assay System (Promega), according to the indications of the manufacturer. Data are expressed as the TOPflash:*Renilla* ratio, relative to the background activity obtained from control untreated cells.

2.6. AChRs pulldown assay and western blot analysis

Surface (S) and intracellular (IC) AChRs expressed on differentiated primary myotubes were collected using biotin-conjugated α-Bungarotoxin (B-BTX) along with streptavidin-agarose beads, as follows. For (S) AChRs collection, myotubes differentiated for 5- or 9-days were washed with ice-cold PBS supplemented with Ca^{2+} and Mg^{2+} (0.6 mM and 1.6 mM, respectively) and then incubated with B-BTX (2 μg/μl) in PBS/Ca^{2+}-Mg^{2+} for 45 min on ice. The unbound B-BTX was washed with ice-cold PBS and cells were collected with a cell scrapper in PBS containing NaF (50 mM), Na_3VO_4 (1 mM) and a protease inhibitors cocktail (Sigma-Aldrich). Cells were collected by mild centrifugation at 8,000x*g* for 5 min at 4 °C. The supernatant was discarded and replaced with cell lysis buffer (Tris-HCl 25 mM pH 8.0, Glycine 25 mM, NaCl 150 mM, EDTA 5 mM and 1% Triton X-100) containing phosphatase and protease inhibitors. Cells were lysed by passing them through a 1-ml syringe with 30 g-needle. The lysates were incubated 10 min on ice and then centrifuged at 15,000x*g* for 15 min at 4 °C. A 10% aliquot from the total sample was stored as the input fraction. Streptavidin-agarose beads were equilibrated in cell lysis buffer and then added to the cell lysate and incubated for 2 h at 4 °C with gently rotation. (S) AChRs were collected by centrifuging agarose beads at 4,000x*g* for 2 min. (IC) AChRs were obtained by re-incubation with B-BTX for 1 h at 4 °C with constantly mixing. The (IC) AChRs-B-BTX complex was collected by incubation with Streptavidin-agarose beads as described above. Input, (S) and (IC) fractions were resolved on 10% SDS-polyacrylamide gels, transferred onto PVDF membranes (Millipore) and subjected to western blot analyses. Antibodies against actin (1:1000, Santa Cruz Biotechnology) as well as against the ε (1:300) or α1 AChRs subunits (1:250, both from Santa Cruz Biotechnology) were incubated 12–15 h at 4 °C or 1 h at room temperature. Bound antibodies were visualized using horseradish peroxidase-coupled secondary antibodies (Jackson ImmunoResearch Laboratories) developed using a chemiluminescence reagent kit (Perkin Elmer).

2.7. Statistical analyses

Data correspond to the average ± SEM of three independent experiments performed by triplicate, except when indicated. Data were statistically analyzed using ANOVA or *t*-test, as indicated in the figure legends.

3. Results and discussion

3.1. Conditions for optimal DNA delivery via electroporation, cell survival and differentiation of mouse satellite cells

Our first aim was to establish the best parameters for transfecting DNA vectors into mouse satellite cells. With this aim, we considered previous reports showing efficient gene transfer of human myoblasts through electroporation [9–11]. In order to achieve efficient electroporation of satellite cells, we used a commercially available system based on capillary and wire type electrodes [13]. This method has proven effective for gene transfer in various cell lines, including

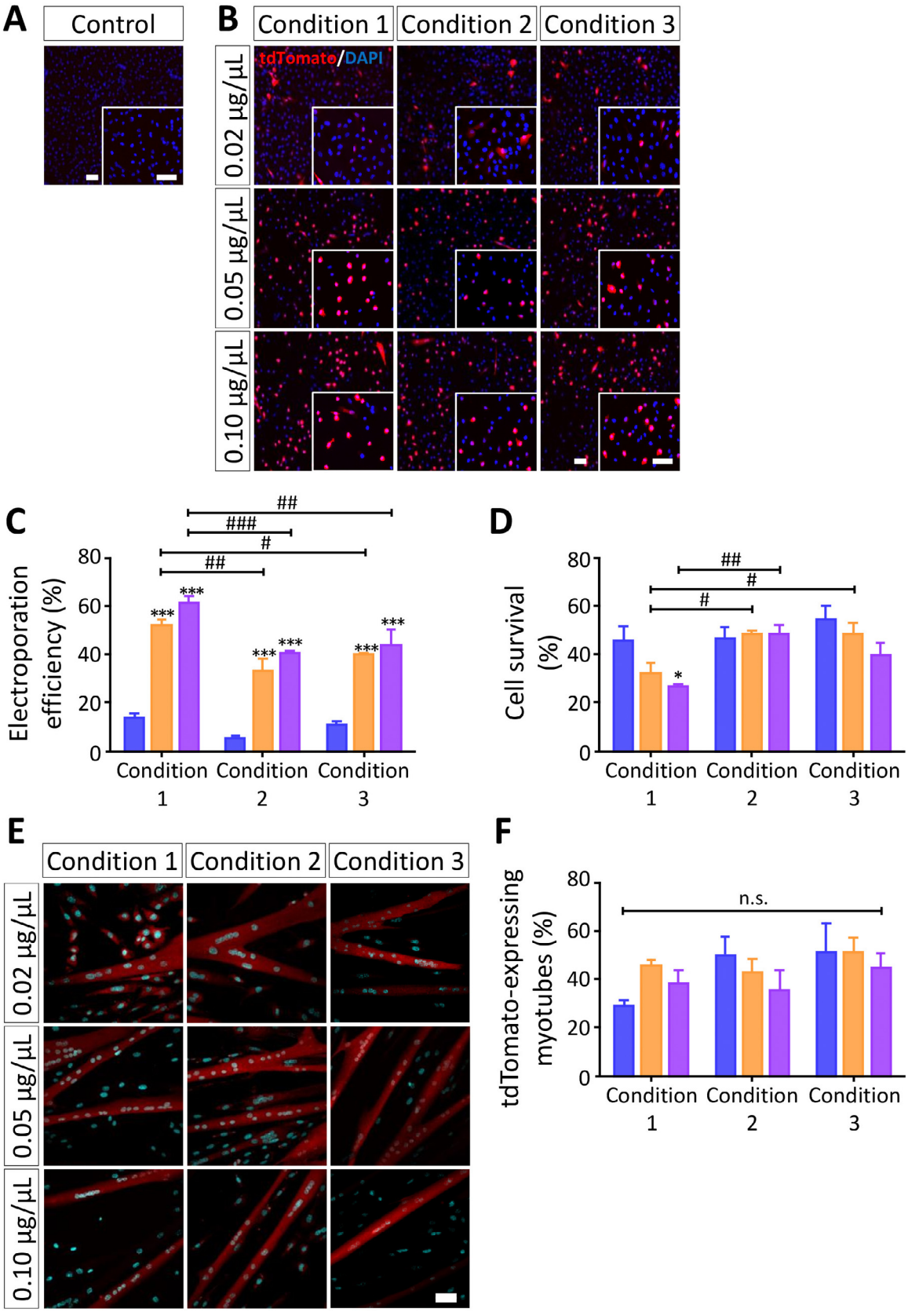
A
Control
B
Condition 1
Condition 2
Condition 3
tdTomato/DAPI
0.02 µg/µL
0.05 µg/µL
0.10 µg/µL
C
Electroporation efficiency (%)
Condition 1
Condition 2
Condition 3
D
Cell survival (%)
E
F
tdTomato-expressing myotubes (%)
n.s.

C2C12 myoblasts [14,15], as well as in primary cells [16]. We used a vector encoding the tdTomato fluorescent protein as it allows analysis of transfection at the cellular level by microscopy. We considered the protocol suggested by the manufacturer to transfect mouse C2C12 myoblasts (condition 1), and the two protocols suggested for rat L6 myoblasts (conditions 2 and 3). Considering the potential toxicity of DNA, we used three DNA concentrations in the mix for each condition (0.02 μg/μl; 0.05 μg/μl, and 0.10 μg/μl). Satellite cells were subjected to the nine selected electroporation conditions. After 24 h, the proportion of electroporated cells was calculated as a percentage of the total cells. As depicted in Fig. 1A-C, low transfection efficiencies were reached with 0.02 μg/μl DNA in each electroporation condition, whereas 0.05 and 0.1 μg/μl DNA gave similar percentages of electroporated cells. Condition 1 yielded the highest electroporation efficiencies, being 52.3 ± 2.0% for 0.05 μg/μl DNA and 61.5 ± 2.6% for 0.1 μg/μl DNA (Fig. 1C). Regarding cell survival, Fig. 1D shows a marked decrease in the number of cells at 0.05 and 0.1 μg/μl DNA in condition 1. In turn, conditions 2 and 3 resulted in around 40–50% cell survival for each tested DNA concentration. According to the manufacturer, our procedure resulted in less transfection efficiency and survival in primary satellite cells than that expected for C2C12 (95% transfection efficiency, 96% viability) and L6 (around 75% efficiency, 90% viability) cell lines. However, our findings are comparable to the quantification of the same parameters after electroporation of human myoblasts [9,11]. In those experiments, the best transfection/survival efficiency ratios were obtained with higher electric field strengths (around 0.8 kV/cm) and with similar DNA concentrations (around 0.05 μg/μl) than the ones we tested [9,11]. Similar to our experiments, another study showed maximal fluorescence intensity (used as a parameter of electroporation efficiency) at 0.6 kV/cm of electric field strength [10]. Some studies have also used lower voltages to apply multiple pulses in order to gradually permeate the myoblast membrane (*i.e.* 8 pulses of 0.2 to 5 ms) [10,11]. As expected with this approach, the better gene transfer efficiencies are reached at expenses of diminishing cell survival. In summary, following our approach, conditions 2 and 3 at 0.05 and 0.1 μg/μl DNA yielded the highest transfection/survival rates, and allowed the successful completion of our subsequent studies on the assembly of postsynaptic structures. We next evaluated the ability of electroporated satellite cells to fuse into multinucleated myotubes. Quantification of the proportion of tdTomato positive myotubes revealed no significant differences between the percentage of transfected myotubes in the three conditions at 0.05 and 0.1 μg/μl DNA. Even though the use of 0.02 μg/μl DNA resulted in low transfection efficiency of mononucleated cells (Fig. 1E and F), the percentage of tdTomato positive myotubes was similar to 0.05 and 0.1 μg/μl DNA in each condition (Fig. 1F). Previous studies with electroporated human myoblasts have also shown the formation of multinucleated cells [9,11]. Remarkably, similar myoblast fusion indexes could be reached after gene transfer through lipofection and electroporation, even though the transfection efficiencies of myoblasts differed with both methods [11]. Therefore, these results suggest that initial differences in the efficiency of gene transfer into myoblasts are compensated upon myotube formation, possibly due to the fusion of transfected with non-transfected satellite cells, which gives rise to an increased proportion of tdTomato-positive myotubes.

3.2. Characterization of aneural postsynaptic structures in electroporated primary myotubes

AChR clustering is a major hallmark of postsynaptic differentiation in muscle cells. Small aggregates of AChRs formed during embryonic developmental stages are converted into bigger and more complex *pretzel*-like postsynaptic structures throughout post-natal NMJ maturation [1,2]. Complex postsynaptic structures, resembling those observed *in vivo*, can also be formed on the surface of C2C12 cells myotubes when cultured onto polyornithine/laminin matrices [8], representing an appropriate aneural *in vitro* model to study the muscle-derived mechanisms controlling the formation and/or maintenance of mature postsynaptic domains. To analyze the assembly of complex postsynaptic structures onto electroporated myotubes, satellite cells subjected to one electroporation condition (0.55 kV/cm, 3 pulses of 10 ms, and 0.5 μg of DNA) were differentiated for 8 days and subsequently stained with BTX to reveal AChR aggregates. In control non-transfected conditions myotubes assembled complex structures (Fig. 2A) that we categorized into *plaques*, *pretzels*, and *fragmented* structures (Fig. 2B). Similar to the control, electroporated myotubes were also able to assemble complex postsynaptic structures (Fig. 2A). Quantification shows that the proportion of postsynaptic structures obtained in control conditions was not significantly different in any of the electroporation conditions (Fig. 2C). Together, these results show that electroporation of muscle cells with a negative control protein does not affect their ability to form myotubes or to assemble complex postsynaptic

Fig. 1. Electroporation efficiency, cell survival and differentiation of mouse primary satellite cells.
Satellite cells obtained from mouse skeletal muscles were electroporated with a plasmid coding for the tdTomato fluorescent protein. Protocols used were: condition 1: 0.55 kV/cm, 3 pulses of 10 ms; condition 2: 0.42 kV/cm, 1 pulse of 30 ms; and condition 3: 0.37 kV/cm, 2 pulses of 30 ms. DNA concentrations of 0.02, 0.05, and 0.1 μg/μl were used in every condition. Control non-electroporated (A) and electroporated (B) satellite cells were counterstained with DAPI to reveal nuclei 24 h post-electroporation. Transfection efficiency (C) is expressed as a proportion of total nuclei. Cell survival (D) was calculated by comparing with the total number of nuclei in non-electroporated cells. (E,F) Control non-electroporated and tdTomato electroporated satellite cells were seeded and differentiated onto polyornithine/laminin coated dishes for eight days (E). The fraction of myotubes expressing the tdTomato fluorescent protein is expressed as a proportion of the total area of myotubes (F). Plots represent the average ± SEM of three independent experiments performed by triplicate. $^{*}p < 0.05$, $^{**}p < 0.01$, $^{***}p < 0.001$, ANOVA. Scale bar = 50 μm.

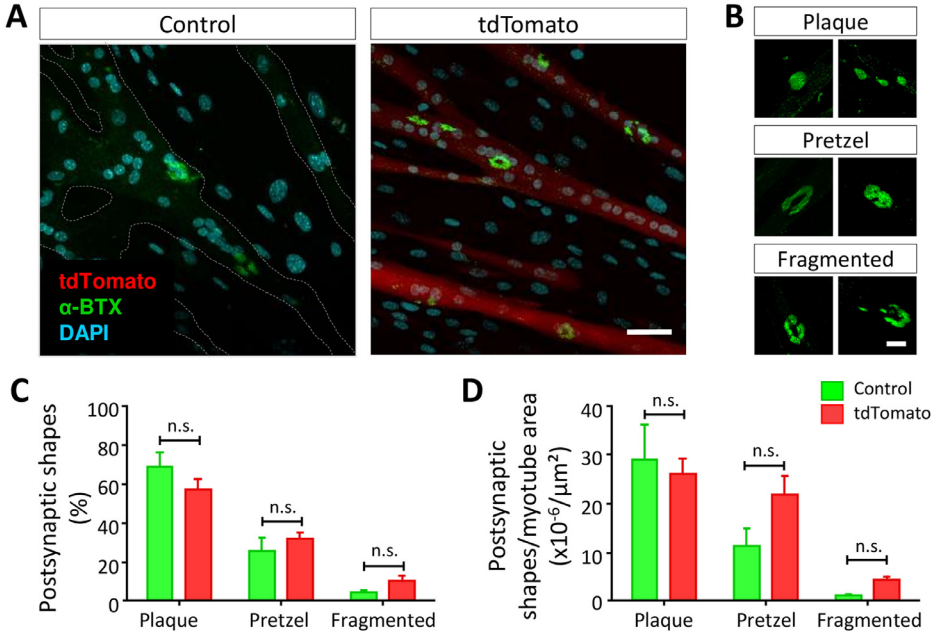

Fig. 2. AChR aggregation in electroporated primary myotubes.
Control non-electroporated and tdTomato electroporated satellite cells were seeded and differentiated onto polyornithine/laminin coated dishes for eight days. Cells were stained with BTX (green) to detect AChRs and DAPI (cyan) to counterstain nuclei (A). AChR aggregates were categorized into *plaque*, *pretzel* or *fragmented* (B). Complex AChR structures were quantified as their relative abundance (C) and as the total number of each category per myotube area (D). Plots represent the average ± SEM of three independent experiments performed by triplicate. n.s. (non-significant) $p > 0.05$, ANOVA. Scale bars = 50 and 10 µm (A and B, respectively).

structures *in vitro*. Similarly, the number of postsynaptic structures per myotube area was not different between control and electroporated myotubes (Fig. 2D).

We next aimed a deeper characterization of the aneural potsynaptic structures formed on the surface of primary myotubes. First, as NMJ postsynaptic domains concentrate subsynaptic myonuclei, we quantified the number of myonuclei within a postsynaptic region of interest and compare with a similar region of interest in other regions of the same myotube (Fig. 3 A, B). Our data show a similar significantly higher proportion of myonuclei in myotube regions containing postsynaptic structures in control and tdTomato electroporated myotubes. These findings confirm previous evidence [8] that presynaptic inputs are not required to concentrate myonuclei in postsynaptic myotube areas (Fig. 3A, B). Second, we analyzed the distribution of rapsyn, a key scaffolding protein of the mature NMJ postsynaptic domain [17]. Immunocytochemical analyses showed that rapsyn co-localized with AChR aggregates in complex postsynaptic structures formed onto control and tdTomato-positive fibers (Fig. 3C), as we observed in antibody control experiments performed in mature NMJs *in vivo* (Fig. 3D). Third, as functional maturation of the NMJ postsynaptic domain involves a switch between the γ and the ε AChR subunits, we next performed AChR pulldown assays and analyzed the presence of the α and ε AChR subunits by Western blot. To this aim, surface receptors of control and electroporated myotubes differentiated for 5 or 9 days were labelled with biotin-conjugated BTX and subsequently precipitated using Streptavidin-agarose beads (Fig. 3E). Western blot analyses of the pulled-down fraction showed comparable amounts of the α AChR subunit in all conditions. Of note, the expression of the postsynaptic organizer protein rapsyn increased from day 5 to day 9 in control and tdTomato-positive myotubes. However, the ε AChR subunit was not detected in the protein fraction

Fig. 3. Characterization of complex AChR aggregates formed on the surface of electroporated myotubes.
Control non-electroporated and tdTomato electroporated satellite cells were seeded and differentiated onto polyornithine/laminin coated dishes for eight days. Myotubes were stained with BTX (green) to detect AChR aggregates and DAPI (cyan) to counterstain nuclei (A). The number of myonuclei within a postsynaptic region of interest was quantified and compared with a similar region of interest in other regions of the same myotube (B). In (C) myotubes were subjected to immunocytochemistry to detect rapsyn (green) and also stained with BTX (white) and DAPI (cyan). The top right panel is a highly magnified image of the dotted line square depicted in the images of the fourth column. (D) Positive anti rapsyn antibody control experiments were performed in mature NMJs from LAL muscles *in vivo*. (E) Control and tdTomato electroporated satellite cells were differentiated for 5 or 9 days. Myotubes were labelled with biotin-conjugated BTX. Total protein extracts were precipitated using Streptavidin-agarose beads and the pulled-down fraction was subjected to Western blot analyses using antibodies to detect the α1 and ε AChR subunits as well as rapsyn (*upper panels*). A fraction of each total myotube lysates was also subjected to Western blot analyses using antibodies to detect the α1 and ε AChR subunits as well as actin (*lower panels*). Scale bars = 20 µm (A), 10 µm (C), and 20 µm (D).

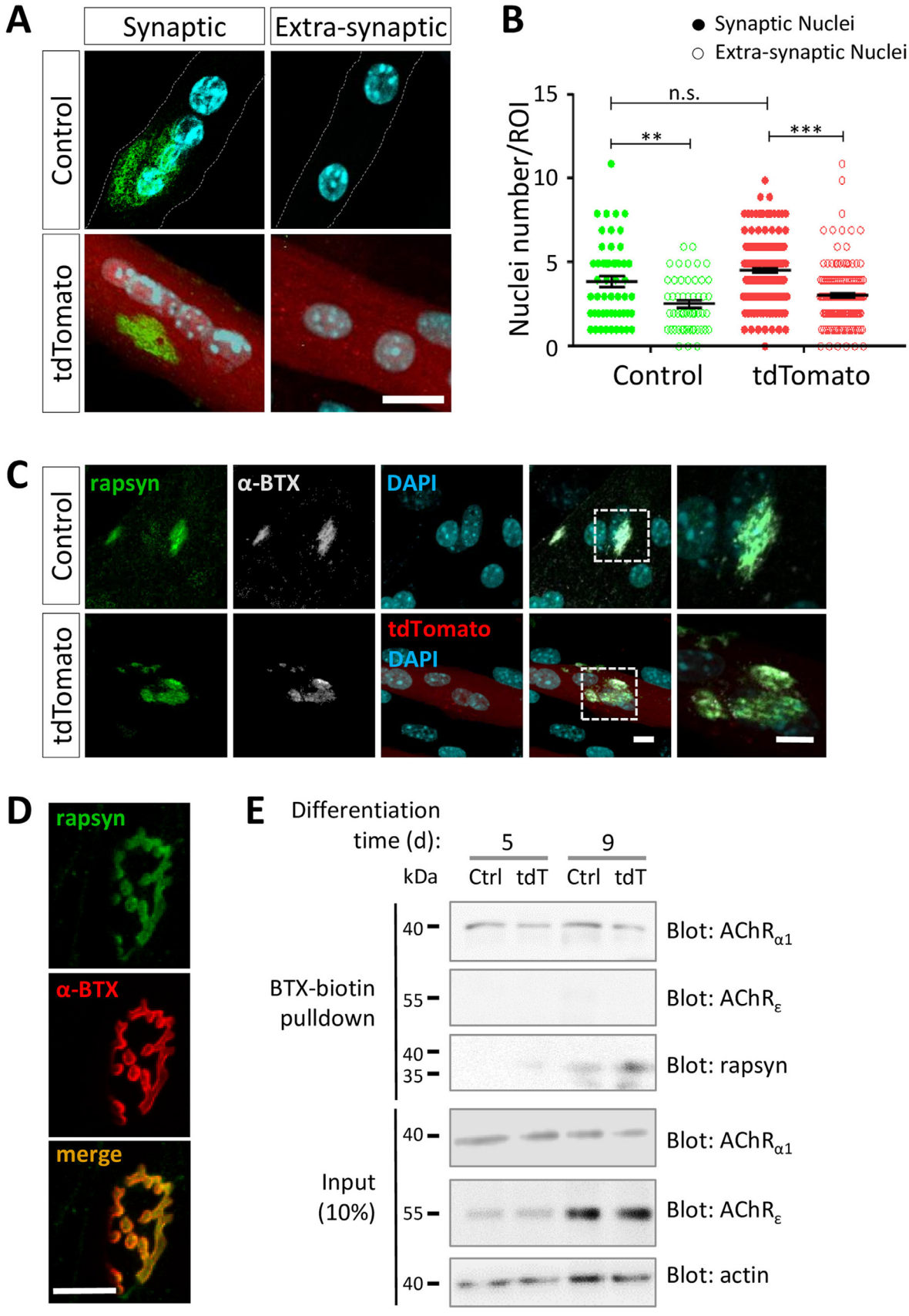
A
Synaptic
Extra-synaptic
Control
tdTomato
B
Synaptic Nuclei
Extra-synaptic Nuclei
Nuclei number/ROI
15
10
5
0
n.s.
**
***
Control
tdTomato
C
Control
tdTomato
rapsyn
α-BTX
DAPI
tdTomato
DAPI
D
rapsyn
α-BTX
merge
E
Differentiation time (d):
5
9
kDa
Ctrl
tdT
Ctrl
tdT
BTX-biotin pulldown
40
55
40
35
Blot: AChR$_{\alpha1}$
Blot: AChR$_{\varepsilon}$
Blot: rapsyn
Input (10%)
40
55
40
Blot: AChR$_{\alpha1}$
Blot: AChR$_{\varepsilon}$
Blot: actin

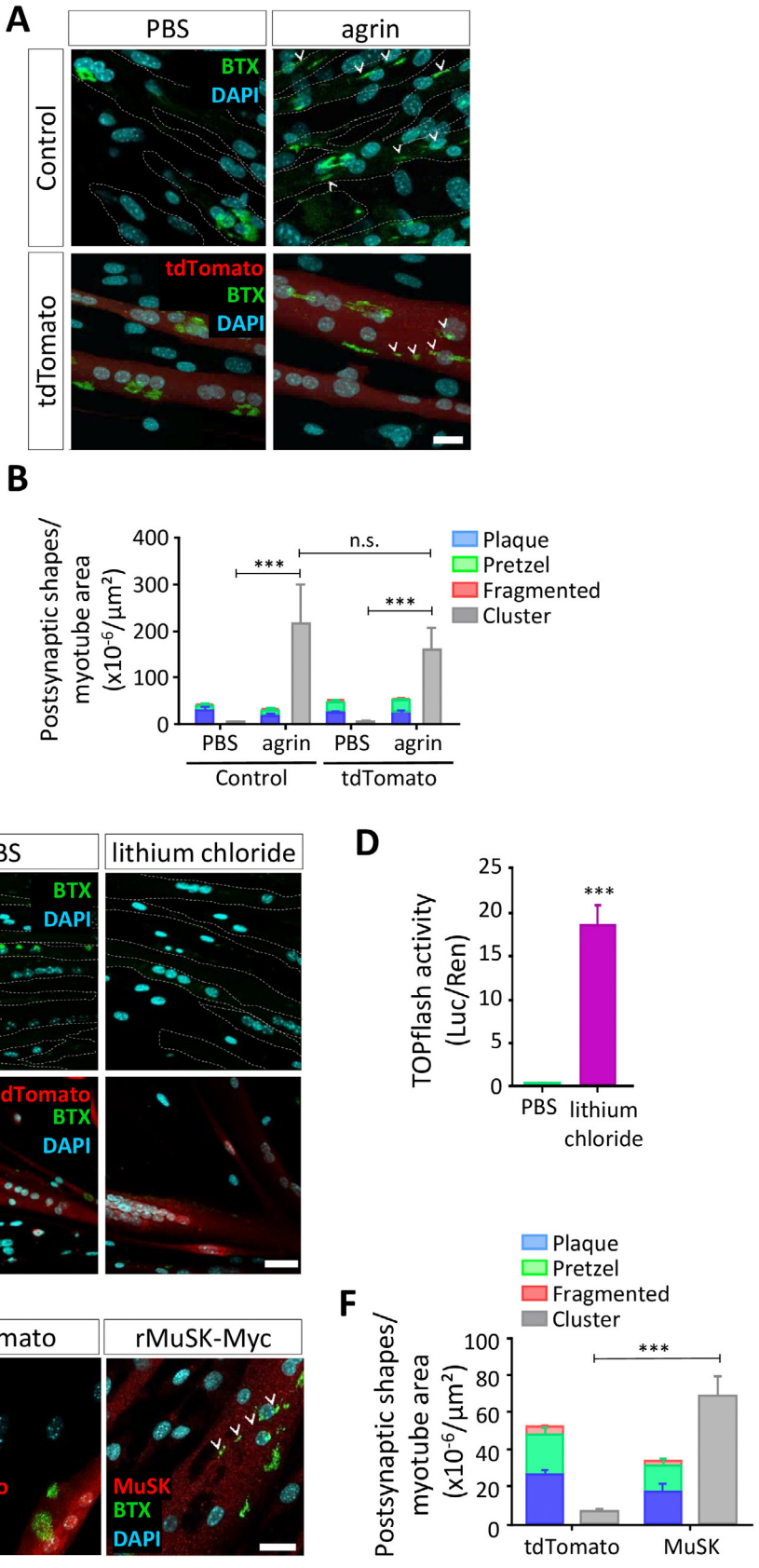
A
PBS
agrin
Control
tdTomato
BTX
DAPI
tdTomato
BTX
DAPI
B
Postsynaptic shapes/
myotube area
(x10-6/µm2)
400
300
200
100
0
***
n.s.
***
Plaque
Pretzel
Fragmented
Cluster
PBS
agrin
PBS
agrin
Control
tdTomato
C
PBS
lithium chloride
Control
tdTomato
BTX
DAPI
tdTomato
BTX
DAPI
D
TOPflash activity
(Luc/Ren)
25
20
15
10
5
0
***
PBS
lithium
chloride
E
tdTomato
rMuSK-Myc
tdTomato
BTX
DAPI
MuSK
BTX
DAPI
F
Plaque
Pretzel
Fragmented
Cluster
Postsynaptic shapes/
myotube area
(x10-6/µm2)
100
80
60
40
20
0
***
tdTomato
MuSK

containing surface biotin-labelled AChRs (Fig. 3E, *upper panels*). In order to rule out if the lack of detection of the ε AChR subunits in the pulled-down fraction was related to its expression, we then analyzed the total expression of the α and ε AChR subunits in fractions of total myotube lysates obtained prior to the pull-down assays. Remarkably, our findings show that myotubes in all conditions express the ε AChR subunit; indeed, myotubes differentiated for 9 days express a higher proportion of this receptor that those differentiated for 5 days (Fig. 3E, *lower panels*). As in the surface-labelled fraction, the expression of the α AChR subunit was similar in all conditions. Similar to our previous experiments, the electroporation procedure or the expression of tdTomato did not affect these parameters (Fig. 3E). It is well known that the switch between the γ and ε AChR subunits that gives rise to functionally mature NMJs is dependent on the presence of active motor axon terminals [18]. Therefore, our present findings reveal that the morphological maturation of postsynaptic structures is independent from its functional maturation, as the latter requires presynaptic inputs. Concurrently, our studies reveal the potential convenience of our *in vitro* preparation to analyze candidate presynaptic signals regulating the functional maturation of the NMJ postsynaptic apparatus.

3.3. Pharmacological modulation of complex postsynaptic structures and functional validation of electroporated genes

The ultimate goals of standardizing this procedure are: (i) to modify the assembly or maintenance of complex postsynaptic structures on muscle cells by (ii) modulating the expression of still unknown muscle-derived functional genes. Based on these notions, we first aimed to induce further AChR aggregation by incubating primary myotubes with agrin, a motor neuron-derived proteoglycan that plays a major role on postsynaptic differentiation *in vivo* and that also induces the formation of small AChR clusters in cultured muscle cells [6,7]. Our results show the formation of typical agrin-induced AChR clusters in both conditions. Interestingly, the strong effect of agrin did not significantly affect the ability of myotubes to form complex postsynaptic structures (Fig. 4A, B). Second, we treated control and tdTomato-expressing myotubes with lithium chloride, as it has proven to inhibit AChR clustering either in normal NMJs *in vivo* [19] or after agrin treatment of cultured myotubes *in vitro* [20]. Our findings show no signs of aneural postsynaptic structures upon lithium treatment in control and electroporated conditions (Fig. 4C). Lithium chloride is a potent inhibitor of GSK3ß [21]. In many cell types, including muscle cells, GSK3ß inhibition leads to the cytosolic accumulation of ß-catenin, followed by its translocation to the nucleus, where it binds to TCF/LEF transcription factors to activate gene expression [22]. In order to address the function of genes expressed in electroporated myotubes, we next subjected mouse satellite cells to electroporation with the TOPflash reporter gene, which contains repeats of the TCF/LEF responsive elements [23] controlling the expression of the *Firefly* luciferase gene. For luciferase activity normalization, myotubes were co-transfected with the pRL-SV40 plasmid, which expresses the *Renilla reniformis* luciferase gene under the control of the constitutive SV40 promoter. After 24 h, lithium chloride was added to the electroporated satellite cells and luciferase activities were measured. Our results show that TOPflash/*Renilla* activation by lithium chloride (18.7 ± 2.2) was more than 50 fold higher than control untreated cells (0.35 ± 0.03) (Fig. 4D). Together, our studies represent a functional validation of electroporated-mediated gene expression in satellite cells. They also show that aneural postsynaptic structures assembled onto electroporated myotubes respond in a similar way to pharmacological treatment than control myotubes do.

Finally, to demonstrate the usefulness of this strategy to modulate the expression of muscle proteins that could affect postsynaptic organization, we electroporated primary satellite cells with a plasmid coding for the muscle-specific tyrosine kinase receptor MuSK, a main postsynaptic organizer [24]. MuSK overexpression caused a significant increase in the number of AChR clusters as compared with the control tdTomato-expressing myotubes (Fig. 4E, F). As upon agrin treatment, the assembly of complex postsynaptic AChR aggregates was not significantly affected by MuSK overexpression. These findings are consistent with previous evidence demonstrating that whereas agrin/MuSK signalling induces the formation of small AChR clusters, laminin-dependent aggregation gives rise to bigger AChR structures following a MuSK-independent mechanism [25]. Our results are also consistent with MuSK overexpression *in vivo* by plasmid DNA microinjection, which resulted in the aggregation of small AChR clusters on the surface of ectopic (*i.e.* extrasynaptic) regions of the muscle fibers [26].

Overall, our proposed method constitutes an easily reproducible and reliable tool to modify the expression of muscle proteins to address their potential role on aneural postsynaptic assembly at the vertebrate NMJ. Gain- and

Fig. 4. Modulation of AChR aggregation and functional analysis of electroporated genes in primary myotubes.
Control non-electroporated and tdTomato electroporated satellite cells were seeded and differentiated onto polyornithine/laminin coated dishes for seven days. Myotubes were treated with 200 pM agrin (A,B) or with 10 mM lithium chloride (C) for 18 h and then stained with BTX (green) to detect AChR aggregates and DAPI (cyan) to counterstain nuclei. Control cells were treated with PBS. AChR aggregates were categorized into *plaque*, *pretzel*, *fragmented* or *cluster* (B). (D) Satellite cells were co-electroporated with TOPflash reporter and *Renilla* plasmids. After 32 h, cells were treated with 50 mM lithium chloride for 15–20 h. Control cells were treated with PBS. The plot shows the Luciferase/*Renilla* ratio (Luc/Ren). (E) Satellite cells were electroporated with the rMuSK-myc plasmid, differentiated for 7 days and triple stained by immunocytochemistry with an anti myc antibody along with BTX (green) and DAPI (cyan) to detect AChR aggregates and nuclei, respectively. Control cells were electropoated with a plasmid coding for tdTomato. (F) Complex AChR structures were quantified and plotted as indicated in (B). Data are expressed as the average ± SEM of three independent experiments performed by quadruplicate ($^{***}p < 0.0001$, paired *t*-test). Scale bar = 50 μm.

loss-of-function experiments using this procedure will help the identification of molecules and mechanisms potentially involved in the early embryonic assembly of AChR clusters, as well as in the maintenance of postsynaptic apparatuses after NMJ denervation, both processes likely controlled by autocrine muscle-derived proteins.

Acknowledgments

Our research has been supported by research grants from FONDECYT 1130321, 1170614 and Millennium Science Initiative (MINREB RC120003) to JPH. JM, VP and DZ are CONICYT fellows. We thank Dr. Sylvain Marcellini for his help with the NEON® system and for permanent support and useful discussion.

Supplementary materials

Supplementary material associated with this article can be found, in the online version, at doi:10.1016/j.nmd.2019.05.005.

References

[1] Marques MJ, Conchello JA, Lichtman JW. From plaque to pretzel: fold formation and acetylcholine receptor loss at the developing neuromuscular junction. J Neurosci 2000;20(10):3663–75.
[2] Sanes JR, Lichtman JW. Induction, assembly, maturation and maintenance of a postsynaptic apparatus. Nat Rev Neurosci 2001;2(11):791–805.
[3] Sanes JR, Lichtman JW. Development of the vertebrate neuromuscular junction. Annu Rev Neurosci 1999;22:389–442.
[4] Witzemann V. Development of the neuromuscular junction. Cell Tissue Res 2006;326(2):263–71.
[5] Fawcett JW, Keynes RJ. Peripheral nerve regeneration. Annu Rev Neurosci 1990;13:43–60.
[6] Bowe MA, Deyst KA, Leszyk JD, Fallon JR. Identification and purification of an agrin receptor from Torpedo postsynaptic membranes: a heteromeric complex related to the dystroglycans. Neuron 1994;12(5):1173–80.
[7] Wallace BG, Nitkin RM, Reist NE, Fallon JR, Moayeri NN, McMahan UJ. Aggregates of acetylcholinesterase induced by acetylcholine receptor-aggregating factor. Nature 1985;315(6020):574–7.
[8] Kummer TT, Misgeld T, Lichtman JW, Sanes JR. Nerve-independent formation of a topologically complex postsynaptic apparatus. J Cell Biol 2004;164(7):1077–87.
[9] Espinos E, Liu JH, Bader CR, Bernheim L. Efficient non-viral DNA-mediated gene transfer to human primary myoblasts using electroporation. Neuromuscul Disord 2001;11(4):341–9.
[10] Lojk J, Mis K, Pirkmajer S, Pavlin M. siRNA delivery into cultured primary human myoblasts–optimization of electroporation parameters and theoretical analysis. Bioelectromagnetics 2015;36(8):551–63.
[11] Mars T, Strazisar M, Mis K, Kotnik N, Pegan K, Lojk J, et al. Electrotransfection and lipofection show comparable efficiency for *in vitro* gene delivery of primary human myoblasts. J Membr Biol 2015;248(2):273–83.
[12] Zahavi EE, Ionescu A, Gluska S, Gradus T, Ben-Yaakov K, Perlson E. A compartmentalized microfluidic neuromuscular co-culture system reveals spatial aspects of GDNF functions. J Cell Sci 2015;128(6):1241–52.
[13] Kim JA, Cho K, Shin MS, Lee WG, Jung N, Chung C, et al. A novel electroporation method using a capillary and wire-type electrode. Biosens Bioelectron 2008;23(9):1353–60.
[14] Cho YD, Yoon WJ, Woo KM, Baek JH, Lee G, Cho JY, et al. Molecular regulation of matrix extracellular phosphoglycoprotein expression by bone morphogenetic protein-2. J Biol Chem 2009;284(37):25230–40.
[15] Miyake M, Hayashi S, Iwasaki S, Chao G, Takahashi H, Watanabe K, et al. Possible role of TIEG1 as a feedback regulator of myostatin and TGF-beta in myoblasts. Biochem Biophys Res Commun 2010;393(4):762–6.
[16] Schumann K, Lin S, Boyer E, Simeonov DR, Subramaniam M, Gate RE, et al. Generation of knock-in primary human T cells using Cas9 ribonucleoproteins. Proc Natl Acad Sci USA 2015;112(33):10437–42.
[17] Gautam M, Noakes PG, Mudd J, Nichol M, Chu GC, Sanes JR, et al. Failure of postsinaptic specialization to develop at neuromuscular junctions of rapsyn-deficient mice. Nature 1995;377(6546):232–6.
[18] Rimer M, Mathiesen I, Lømo T, UJ M. g-AChR/e-AChR switch at agrin-induced postsynaptic-like apparatus in skeletal muscle. Mol Cell Neurosci 1997;9:254–63.
[19] Pestronk A, Drachman DB. Lithium reduces the number of acetylcholine receptors in skeletal muscle. Science 1980;210(4467):342–3.
[20] Sharma SK, Wallace BG. Lithium inhibits a late step in agrin-induced AChR aggregation. J Neurobiol 2003;54(2):346–57.
[21] Stambolic V, Ruel L, Woodgett JR. Lithium inhibits glycogen synthase kinase-3 activity and mimics wingless signalling in intact cells. Curr Biol 1996;6(12):1664–8.
[22] Miller JR, Moon RT. Signal transduction through beta-catenin and specification of cell fate during embryogenesis. Genes Dev 1996;10(20):2527–39.
[23] Veeman MT, Slusarski DC, Kaykas A, Louie SH, Moon RT. Zebrafish prickle, a modulator of noncanonical Wnt/Fz signaling, regulates gastrulation movements. Curr Biol 2003;13(8):680–5.
[24] DeChiara TM, Bowen DC, Valenzuela DM, Simmons MV, Compton DL, Rojas E, et al. The receptor tyrosine kinase musk is required for neuromuscular junction formation in vivo. Cell 1996;85:501–12.
[25] Sugiyama JE, Glass DJ, Yancopoulos GD, Hall ZW. Laminin-induced acetylcholine receptor clustering: an alternative pathway. J Cell Biol 1997;139(1):181–91.
[26] Sander A, Hesser BA, Witzemann V. MuSK induces *in vivo* acetylcholine receptor clusters in a ligand-independent manner. J Cell Biol 2001;155(7):1287–96.